Article

Chiral Rodlike Platinum Complexes, Double Helical Chains, and Potential Asymmetric Hydrogenation Ligand Based on "Linear" Building Blocks: 1,8,9,16-Tetrahydroxytetraphenylene and 1,8,9,16-Tetrakis(diphenylphosphino)tetraphenylene

Hai-Yan Peng, Chi-Keung Lam, Thomas C. W. Mak, Zongwei Cai, Wai-Tang Ma, Yu-Xue Li, and Henry N. C. Wong

J. Am. Chem. Soc., **2005**, 127 (26), 9603-9611• DOI: 10.1021/ja051013l • Publication Date (Web): 10 June 2005

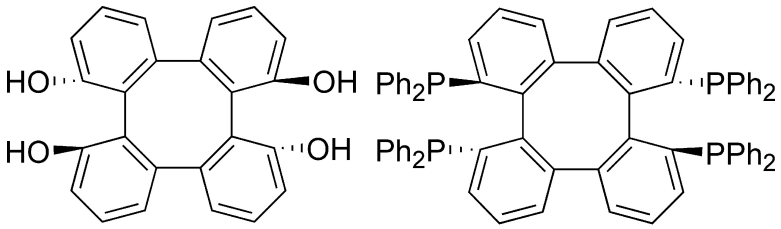

(*R,R*)-**3a** (*S,S*)-**3b**

More About This Article

Additional resources and features associated with this article are available within the HTML version:

- Supporting Information
- Links to the 10 articles that cite this article, as of the time of this article download
- Access to high resolution figures
- Links to articles and content related to this article
- Copyright permission to reproduce figures and/or text from this article

View the Full Text HTML

J|A|C|S
ARTICLES
Published on Web 06/10/2005

Chiral Rodlike Platinum Complexes, Double Helical Chains, and Potential Asymmetric Hydrogenation Ligand Based on "Linear" Building Blocks: 1,8,9,16-Tetrahydroxytetraphenylene and 1,8,9,16-Tetrakis(diphenylphosphino)tetraphenylene

Hai-Yan Peng,[†] Chi-Keung Lam,[‡] Thomas C. W. Mak,[‡] Zongwei Cai,[§] Wai-Tang Ma,[§] Yu-Xue Li,[||] and Henry N. C. Wong*,[†,‡]

Contribution from the Shanghai-Hong Kong Joint Laboratory in Chemical Synthesis and The State Key Laboratory of Organometallic Chemistry, Shanghai Institute of Organic Chemistry, The Chinese Academy of Sciences, 354 Feng Lin Road, Shanghai 200032, China, Department of Chemistry, The Chinese University of Hong Kong, Shatin, New Territories, Hong Kong SAR, China, and Department of Chemistry, Hong Kong Baptist University, Kowloon Tong, Kowloon, Hong Kong SAR, China

Received February 17, 2005; E-mail: hncwong@cuhk.edu.hk

Abstract: This paper is concerned with the synthesis of 1,8,9,16-tetrahydroxytetraphenylene (**3a**) via copper(II)-mediated oxidative coupling, its resolution to optical antipodes, and its conversion to 1,8,9,16-tetrakis(diphenylphosphino)tetraphenylene (**3b**). On the basis of these chiral "linear" building blocks, three rodlike chiral complexes, triblock (*R*,*R*,*R*,*R*)-**17** and (*S*,*S*,*S*,*S*)-**20** and pentablock (*R*,*R*,*R*,*R*,*R*,*R*,*R*,*R*)-**22**, were constructed. As a hydrogen bond donor, racemic and optically active **3a** was allowed to assemble with linear acceptors to afford highly ordered structures. A 1:1 adduct of 4,4′-bipyridyl and (±)-**3a** exists in a dimeric form of **3a** linked by 4,4′-bipyridyl through hydrogen bonds. Pyrazine serves as a short linker between achiral parallel chains each formed by (±)-**3a**, while self-assembly of homochiral **3a** into alternate parallel chains occurs in the adduct of 5,5′-dipyrimidine with (±)-**3a**. Self-assembly of (*S*,*S*)-**3a** or (*R*,*R*)-**3a** with 4,4′-dipyridyl yielded a packing of chiral double helical chains formed by chiral tetrol **3a** molecules. A novel chiral ligand, (*S*,*S*)-**23**, derived from **3a** was used in the asymmetric catalytic hydrogenation of α-acetamidocinnamate, yielding up to 99.0% ee and 100% conversion.

Introduction

Tetraphenylene (**1**) and its derivatives[1−6] form interesting clathrate inclusion compounds[2,3] and exhibit interesting electronic properties.[4,6b] Due to the high barrier for inversion of the central cyclooctatetraene ring of **1**,[5] chiral tetraphenylenes can be realized although very few nonracemic tetraphenylene derivatives[6] are known. It is therefore of interest to prepare optically active tetraphenylenes, which may be employed as chiral building blocks[7−9] for 3-dimensional scaffold construction. A program has been initiated in our laboratories in the syntheses of building blocks **2**−**6**. It is noteworthy that **2**,[10a] **3,** and **5** are chiral while **4**[10b] and **6**[10c] are achiral. Geometrically, **3** is a linear unit containing reactive sites which point in opposite directions, while the reactive sites of **4** are orientated at an idealized angle

[†] Shanghai-Hong Kong Joint Laboratory in Chemical Synthesis, Shanghai Institute of Organic Chemistry.
[‡] The Chinese University of Hong Kong.
[§] Hong Kong Baptist University.
[||] The State Key Laboratory of Organometallic Chemistry, Shanghai Institute of Organic Chemistry.

(1) Rapson, W. S.; Shuttleworth, R. G.; van Niekerk, J. N. *J. Chem. Soc.* **1943**, 326−327.
(2) For reviews, see: (a) Mak, T. C. W.; Wong, H. N. C. *Top. Curr. Chem.* **1987**, *140*, 141−164. (b) Mak, T. C. W.; Wong, H. N. C. In *Comprehensive Supramolecular Chemistry*; MacNicol, D. D., Toda, F., Bishop, R., Eds.; Pergamon Press: Oxford, 1996; Vol. 6, pp 351−369.
(3) (a) Man, Y. M.; Mak, T. C. W.; Wong, H. N. C. *J. Org. Chem.* **1990**, *55*, 3214−3221. (b) Wong, H. N. C.; Man, Y. M.; Mak, T. C. W. *Tetrahedron Lett.* **1987**, *28*, 6359−6362. (c) Huang, N. Z.; Mak, T. C. W. *J. Chem. Soc., Chem. Commun.* **1982**, 543−544. (d) Schwager, H.; Spyroudis, S.; Vollhardt, K. P. C. *J. Organomet. Chem.* **1990**, *382*, 191−200.
(4) Scholz, M.; Gescheidt, G. *J. Chem. Soc., Perkin Trans. 2* **1994**, 735−740.
(5) Rashidi-Ranjbar, P.; Man, Y. M.; Sandström, J.; Wong, H. N. C. *J. Org. Chem.* **1989**, *54*, 4888−4892.
(6) (a) Rajca, A.; Safronov, A.; Rajca, S.; Shoemaker, R. *Angew. Chem., Int. Ed. Engl.* **1997**, *36*, 488−491. (b) Rajca, A.; Safronov, A.; Rajca, S.; Wongsriratanakul, J. *J. Am. Chem. Soc.* **2000**, *122*, 3351−3357. (c) Rajca, A.; Wang, H.; Bolshov, P.; Rajca, S. *Tetrahedron Lett.* **2001**, *57*, 3725−3735.
(7) (a) Lehn J.-M. *Science* **1985**, *227*, 849−856. (b) *Comprehensive Supramolecular Chemistry*; Lehn, J.-M., Chair Ed.; Atwood, J. L., Davies, J. E. D., MacNicol, D. D., Vögtle, F., Executive Eds.; Pergamon Press: Oxford, 1996.
(8) (a) Baxter, P. N. W. In *Comprehensive Supramolecular Chemistry*; Sauvage, J.-P., Hosseini, M. W., Eds.; Pergamon Press: Oxford, 1996; Vol. 9, pp 65−212. (b) Fujita, M. In *Comprehensive Supramolecular Chemistry*; Sauvage, J.-P., Hosseini, M. W., Eds.; Pergamon Press: Oxford, 1996; Vol. 9, pp 253−282. (c) Leininger, S.; Olenyuk, B.; Stang, P. J. *Chem. Rev.* **2000**, *100*, 853−908. (d) Olenyuk, B.; Fechtenkötter, A.; Stang, P. J. *J. Chem. Soc., Dalton Trans.* **1998**, 1707−1728. (e) Stang, P. J.; Olenyuk, B. *Acc. Chem. Res.* **1997**, *30*, 502−518. (f) Fujita, M. *Chem. Soc. Rev.* **1998**, *27*, 417−425.
(9) Jiang, H.; Lin, W. *J. Am. Chem. Soc.* **2003**, *125*, 8084−8085.
(10) (a) Wen, J.-F.; Hong, W.; Yuan, K.; Mak, T. C. W.; Wong, H. N. C. *J. Org. Chem.* **2003**, *68*, 8918−8931. (b) Hui, C. W.; Mak, T. C. W.; Wong, H. N. C. *Tetrahedron* **2004**, *60*, 3523−3531. (c) Lai, C. W.; Chi, K.; Hung, K.; Mak, T. C. W.; Wong, H. N. C. *Org. Lett.* **2003**, *5*, 823−826.

Scheme 1

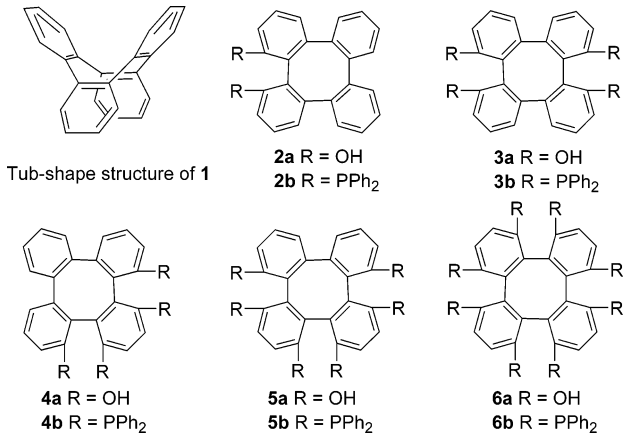

of 90° (Scheme 1). In this manner, the functional groups of these building blocks could be interconnected with guest molecules via noncovalent interaction,[7,8] or with central metal linkages via covalent interaction,[7−9] forming ordered linear, 2- and 3-dimensional scaffolds. Herein we report the synthesis of optically active 1,8,9,16-tetrahydroxytetraphenylene (**3a**) and 1,8,9,16-tetrakis(diphenylphosphino)tetraphenylene (**3b**). On the basis of the linear property of **3**, chiral rodlike platinum complexes were constructed, while self-assembly of **3a** formed double helical chains through hydrogen bonds. An effective chiral ligand, (*S*,*S*)-**23**, derived from **3a** was also employed in the asymmetric catalytic hydrogenation of α-acetamidocinnamate. This linear ligand is the first example of a tetraphenylene backbone introduced into an effective catalytic ligand as a source of chirality.

Results and Discussion

Synthesis of 1,8,9,16-Tetrahydroxytetraphenylene (3a) and 1,8,9,16-Tetrakis(diphenylphosphino)tetraphenylene (3b). One way to synthesize tetraphenylenes is via copper(II)-mediated oxidative coupling.[13−15] This approach was adopted in our synthesis and resolution of **3a**, the procedures being shown in Scheme 2. Thus, the iodination of **7**[11] afforded **8**,[12] whose oxidative coupling via its corresponding lithium salt[13−15] led to the formation of a mixture of compounds, whose careful chromatography resulted in the separation of a product in a disappointing yield of 13%. This compound exhibited strong signals at *m*/*z* 424 in its mass spectrum. Elemental analysis and the mass spectrum combine to indicate the molecular formula of **9**. The structure of **9** was also supported by its ^{1}H NMR spectrum (300 MHz, $CDCl_3$), which exhibited a singlet at δ 3.65 ppm that can be assigned to the four methoxy groups. Moreover, three AMX-type doublets of doublets centered at δ 7.19 ppm (J = 7.6, 8.2 Hz), 6.86 ppm (J = 1.1, 7.6 Hz), and 6.79 ppm (J = 1.1, 8.2 Hz) can be attributed to three types of protons in the benzene rings. The molecular ion peak of compound **9** in its EI mass spectrum was observed at *m*/*z* 424.16888, which is in good agreement with the theoretical value of 424.16746 for the molecular formula $C_{28}H_{24}O_4$ of **9**. Optimization procedures revealed that the presence of tetramethylethylenediamine (TMEDA) was crucial to the coupling while the change of *n*-BuLi to *t*-BuLi or $CuCl_2$ to $CuBr_2$ showed very little influence. After repeated trials of employing different equivalents of TMEDA, it was eventually found that the presence of 2 equiv of TMEDA resulted in the formation of **9** in the best yield of 29%.

The demethylation of **9** with boron tribromide yielded **3a**, whose structure was determined by spectroscopic methods and was also confirmed by an X-ray study (Figure 1). NMR spectroscopy and MS, as well as elemental analysis, are in full agreement with the assigned structure. The highly symmetrical structure of **3a** can be demonstrated by the appearance of only one singlet at δ 8.74 ppm for the hydroxyl proton and three AMX-type doublets of doublets centered at δ 6.97 (dd, J = 7.5, 8.0 Hz), 6.62 (d, J = 8.0 Hz), and 6.55 (d, J = 7.5 Hz)

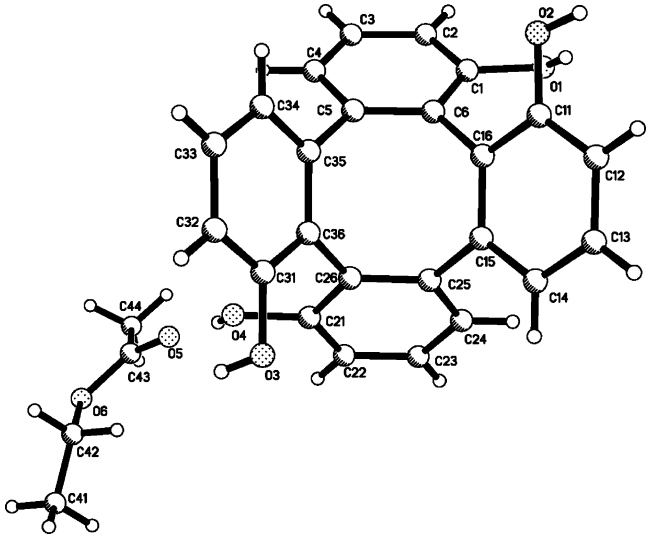

Figure 1. ORTEP drawing of **3a** (solvent EtOAc).

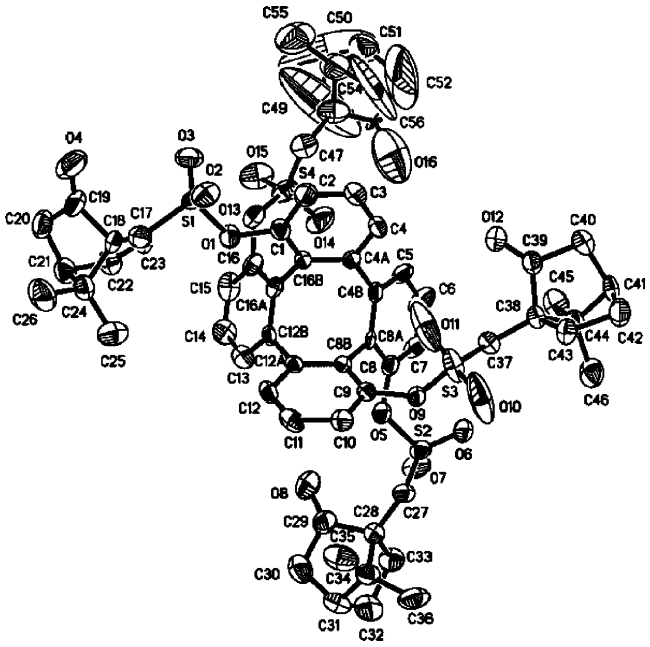

Figure 2. ORTEP drawing of **10**.

(11) Baker, W.; Barton, J. W.; McOmie, J. F. W. *J. Chem. Soc.* **1958**, 2658−2663.
(12) Cereghetli, M.; Schmid, R.; Schonhner, P.; Rageot, A. *Tetrahedron Lett.* **1996**, *37*, 5343−5346.
(13) Rajca, A.; Wang, H.; Bolshov, P.; Rajca, S. *Tetrahedron* **2001**, *57*, 3725−3735.
(14) Kabir, S. M. H.; Iyoda, M. *Synthesis* **2000**, *13*, 1839−1842.
(15) Kabir, S. M. H.; Hasegawa, M.; Kuwatani, Y.; Yoshia, M.; Matsuyama, H.; Iyoda, M. *J. Chem. Soc., Perkin Trans. 1* **2001**, 159−165.

Scheme 2

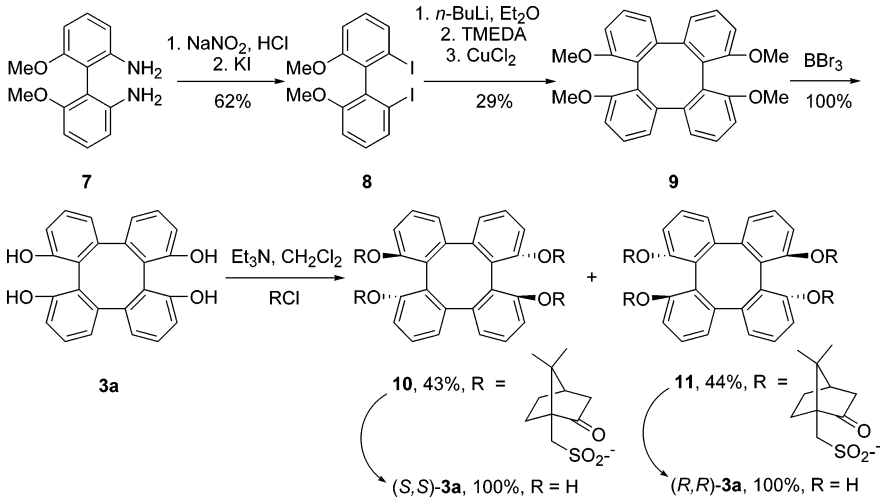

Scheme 3

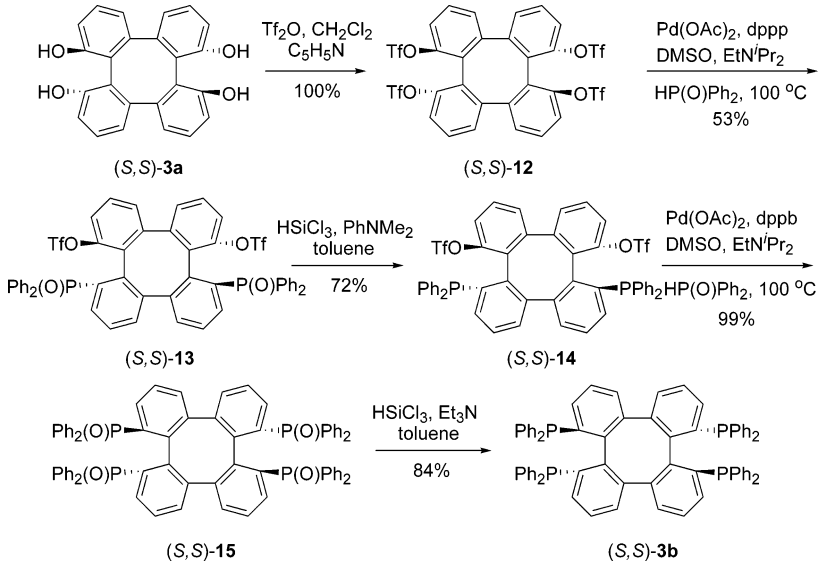

ppm for benzene protons. Carbon-13 signals appear at δ 154.2, 143.8, 127.1, 124.2, 118.5, and 113.4 ppm in d_6-DMSO. The molecular ion peak of compound **3a** in its EI mass spectrum was observed at *m*/*z* 368.10044, which is in good agreement with the theoretical value of 368.10049 for the molecular formula $C_{24}H_{16}O_4$ of **3a**. The resolution of **3a** was performed through (*S*)-camphorsulfonylation.[16] It was also found that the diastereomeric tetrakis-(*S*)-camphorsulfonates of (±)-**3a**, namely, **10** and **11**, were chromatographically separable using a 3:1 mixture of benzene and ethyl acetate as an eluent mixture. Due to the fact that the absolute configuration of the (*S*)-camphorsulfonyl group is defined, an X-ray crystallographic analysis of the less polar biscamphorsulfonate **10** therefore led us to confirm the absolute structure of its appended **3a** to be of (*S*,*S*)-configuration (Figure 2). In this manner, the absolute stereochemistry of **11** with an appended (*R*,*R*)-**3a** was also indirectly confirmed. A subsequent desulfonylation generated the enantiomerically pure (*S*,*S*)-**3a** and (*R*,*R*)-**3a**. The former showed a negative first Cotton effect at 286 nm and a positive second Cotton effect at 236 nm, while the latter exhibited a positive first Cotton effect at 286 nm and a negative second Cotton effect at 236 nm as can be seen in the Supporting Information. Compound (*S*,*S*)-**3a** exhibited a specific rotation of $[\alpha]^{20}_D$ −55.8 (MeOH, $c = 1.05$), which is opposite to that of (*R*,*R*)-**3a**, $[\alpha]^{20}_D$ +55.3 (MeOH, $c = 1.07$).

The quest for substituted tetraphenylenes that contain other functional groups as metal coordination sites promoted us to undertake the transformation of hydroxyl groups of **3a** to **3b** (Scheme 3). Thus, compound (*S*,*S*)-**3a** was readily converted into the triflate (*S*,*S*)-**12** with triflic anhydride in the presence of pyridine. The palladium-catalyzed phosphinylation of (*S*,*S*)-**12** with diphenylphospine oxide proceeded smoothly.[18] Although in theory three diphosphinylated products may be formed, only (*S*,*S*)-**13** was detected, whose structure was determined by X-ray studies (Figure 3). Reduction of (*S*,*S*)-**13** by trichlorosilane gave the corresponding phosphine (*S*,*S*)-**14**.[19] A second phosphinylation of (*S*,*S*)-**14** led to the desired tetraphosphinyltetraphenylene (*S*,*S*)-**15**,[18] as depicted in Figure 4. Reduction of (*S*,*S*)-**15** with trichlorosilane[19] eventually furnished (*S*,*S*)-**3b** in a total

(16) Chow, H.-F.; Wan, C.-W.; Ng, M.-K. *J. Org. Chem.* **1996**, *61*, 8712−8714.

(17) See the Supporting Information.

(18) Xie, J.-H.; Wang, L.-X.; Fu, Y.; Zhu, S.-F.; Fang, B.-M.; Duan, H.-F.; Zhou, Q.-L. *J. Am. Chem. Soc.* **2003**, *125*, 4404−4405.

(19) Takaya, H.; Akutagawa, S.; Noyori, R. *Org. Synth.* **1989**, *67*, 20−30.

Scheme 4

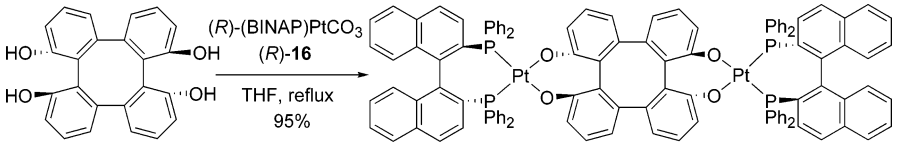

yield of 32%. Only one peak at δ −13.2 ppm in its ^{31}P NMR spectrum (121.5 MHz, C_6D_6) proved that this is a signal for a trivalent phosphine. A protonated molecular ion peak of compound **3b** in its ESI mass spectrum was observed at *m*/*z* 1041.3092, which is in good agreement with the theoretical value of 1041.3073 for its molecular formula $C_{72}H_{53}P_4$. Compound (*S*,*S*)-**3b** showed a specific rotation of $[\alpha]^{20}_D$ +62.1 (CH_2Cl_2, c = 0.33). In a similar manner, (*R*,*R*)-**3b** was also realized,which gave$[\alpha]^{20}_D$ −64.0 (CH_2Cl_2, c = 1.10).

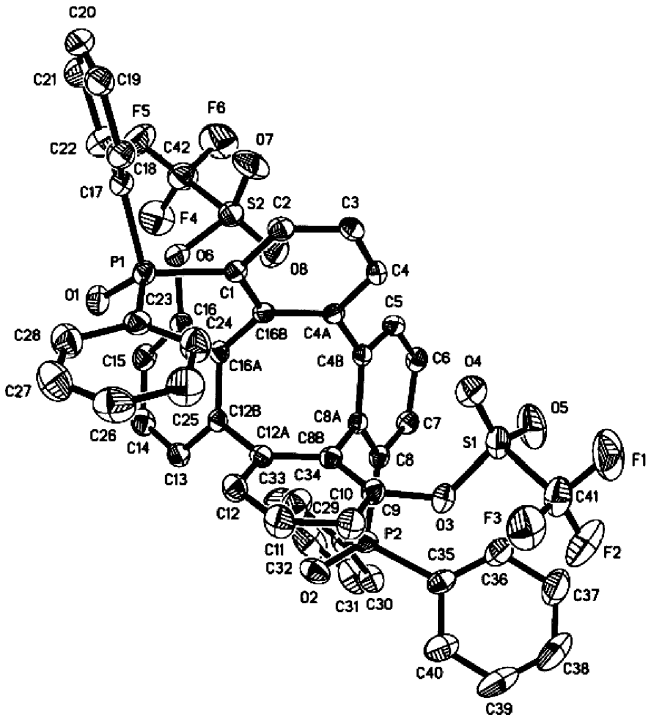

Figure 3. ORTEP drawing of **13**.

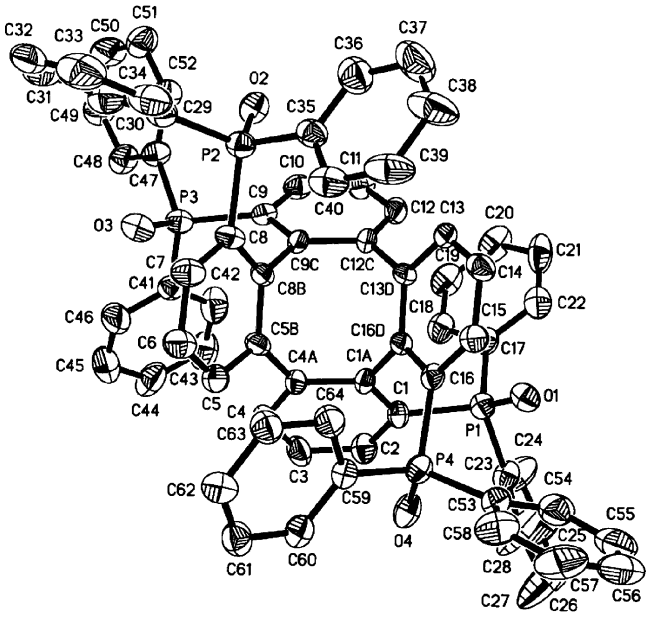

Figure 4. ORTEP drawing of **15**.

Scheme 5

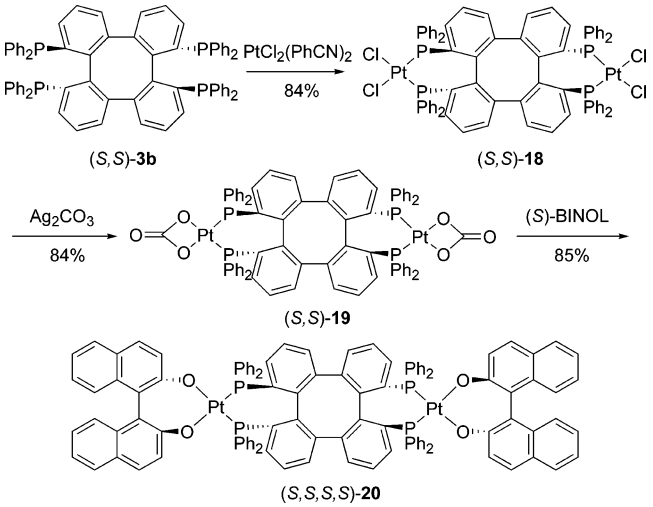

Formation of Chiral Rodlike Platinum Complexes. With (*S*,*S*)-**3a**, (*R*,*R*)-**3a**, (*S*,*S*)-**3b**, and (*R*,*R*)-**3b** in hand, we then explored the possibilities for the formation of chiral platinum complexes. The reaction of (*R*,*R*)-**3a** with 2 equiv of (*R*)-(BINAP)$PtCO_3$ (**16**)[10a,20] afforded a symmetrical complex showing a single peak at δ 4.90 ppm (J_{Pt-P} = 3655 Hz) in its ^{31}P NMR spectrum. The structure of this complex can be assigned as (*R*,*R*,*R*,*R*)-**17**, as depicted in Scheme 4. The protonated molecular ion peak of compound **17** in its ESI-TOF mass spectrum[17] was observed at *m*/*z* 1999.4169, which is in good agreement with the theoretical value of 1999.4072 for the molecular formula $C_{112}H_{77}O_4P_4{}^{195}Pt_2$. The enantiomer, namely, (*S*,*S*,*S*,*S*)-**17**, was also accordingly realized, and provided $[\alpha]^{20}_D$ −796 (THF, c = 0.28), which is opposite to that of (*R*,*R*,*R*,*R*)-**17**, $[\alpha]^{20}_D$ +788 (CH_2Cl_2, c = 1.23).

Another triblock platinum complex utilizing (*S*,*S*)-**3b** as the central building framework was also synthesized (Scheme 5). First, the conversion of (*S*,*S*)-**3b** to its platinum complex resulted in (*S*,*S*)-**18**, which was converted to platinum carbonate (*S*,*S*)-**19**.[10a,20] In a similar manner, (*R*,*R*)-**19** was also obtained from (*R*,*R*)-**3b**. The reaction of (*S*,*S*)-**19** with 2 equiv of (*S*)-BINOL afforded a symmetric triblock complex, (*S*,*S*,*S*,*S*)-**20**,[10a,20] whose structure was substantiated by MS[17] and microanalysis, as well as by ^{1}H and ^{31}P NMR spectroscopy, which exhibited only one singlet at δ 2.33 ppm (J_{Pt-P} = 3655 Hz). The protonated molecular ion peak of compound **20** in its ESI-TOF mass spectrum was observed at *m*/*z* 1999.4211, matching the theoretical value of 1999.4072 for the molecular formula $C_{112}H_{77}O_4P_4{}^{195}Pt_2$.

(20) Tudor, M. D.; Becker, J. J.; White, P. S.; Gagné, M. R. *Organometallics* **2000**, *19*, 4376−4380.

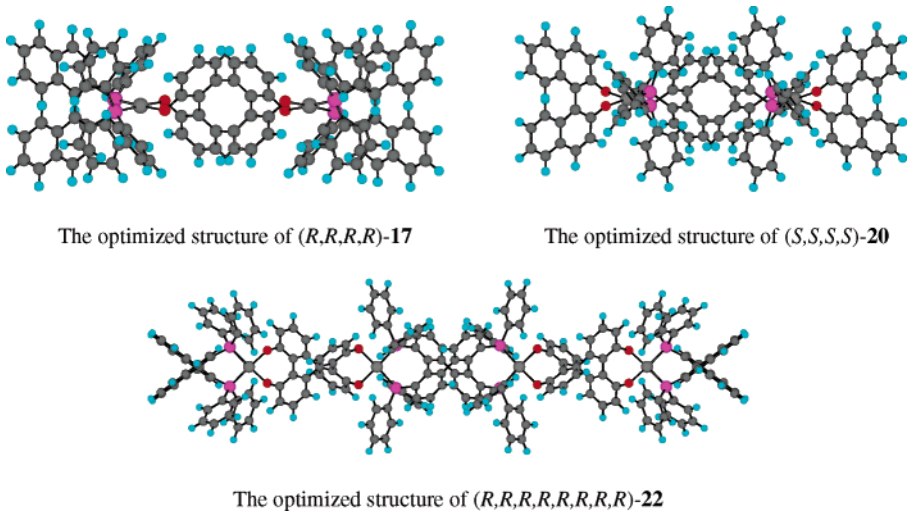

Figure 5. Optimized structures of **17**, **20**, and **22**.

Scheme 6

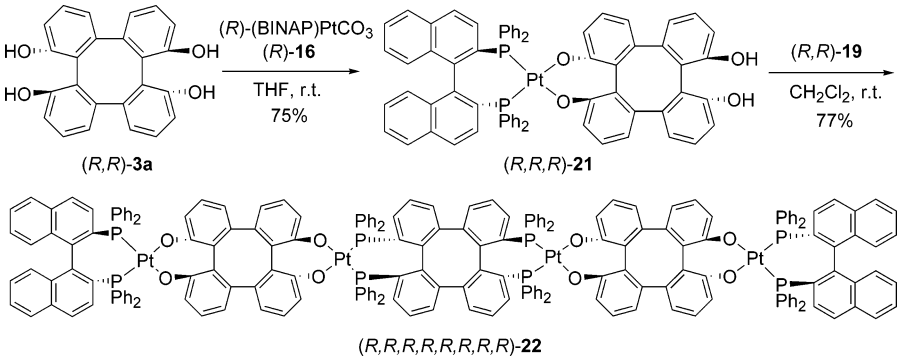

Eventually, a pentablock chiral platinum complex was realized on the basis of the aforementioned results. The reaction of (*R*,*R*)-**3a** at room temperature with 1 equiv of (*R*)-(BINAP)-$PtCO_3$ (**16**) gave (*R*,*R*,*R*)-**21** in a yield of 75%.[10a,20] Then 1 equiv of (*R*,*R*)-**19** was allowed to react at room temperature with 2 equiv of (*R*,*R*,*R*)-**21**, leading to a symmetrical complex with only two singlets seen at δ 10.41 (J_{Pt-P} = 3661 Hz) and 5.07 (J_{Pt-P} = 3702 Hz) ppm in its ^{31}P NMR spectrum. The IR spectrum of this complex demonstrates the disappearance of the characteristic strong absorptions of the C=O double bond at 1672 and 1622 cm^{-1} as detected for (*S*,*S*)-**19**. Element analysis and mass spectrometric analysis led us to assign the molecular formula of (*R*,*R*,*R*,*R*,*R*,*R*,*R*,*R*)-**22** to this complex, as shown in Scheme 6. Complex **22** was analyzed by using matrix-assisted laser desorption/ionization time-of-flight mass spectrometry (MALDI-TOFMS) with dithranol as matrix. The protonated molecular ion peak of compound **22** was observed at *m*/*z* 3795.4 with a small peak intensity. Fragment ions at *m*/*z* 850.172 and 1182.250 were also detected with their accurate masses and isotope patterns matching the theoretical values for the molecular formulas of $C_{44}H_{34}P_2O_2{}^{195}Pt$ and $C_{68}H_{46}P_2O_4{}^{195}Pt$, respectively.

Unfortunately, attempts to obtain single crystals of complexes **17**, **20**, and **22** have so far been unfruitful. To have a better understanding of these rodlike structures, density functional studies have been performed with the Gaussian 98 program.[21a] For C and H, the 3-21G basis set was used, for O and P, the 6-31G(d) basis set was used, and for Pt, the Lanl2DZ basis set with an effective core potential (ECP)[21b] was used. These models were fully optimized with the B3LYP[21c-e] method. In this manner, the symmetry and the dimensions (nm) of **17**, **20**, and **22** are shown in Table 1. The optimized structures of **17**, **20**, and **22** were all rodlike in nanoscale (Figure 5).[21d]

Table 1. Symmetry and the Dimensions (nm) of **17**, **20**, and **22**

		dimensions (nm)		
structure	symmetry	length	width	height
(*R*,*R*,*R*,*R*)-**17**	D_2	2.5776	1.2684	0.9606
(*S*,*S*,*S*,*S*)-**20**	D_2	2.5684	1.3446	1.1906
(*R*,*R*,*R*,*R*,*R*,*R*,*R*,*R*)-**22**	D_2	4.7502	1.1640	1.3448

Supramolecular Assembly of (±)-3a and (*S*,*S*)-3a with Hydrogen Bond Acceptors. With reference to the "saddle"-like structure of tetrol **3a**, it can be seen that the hydroxyl groups on the C-1 and C-16 positions are close to each other, and so are those on the C-8 and C-9 positions. The two pairs of hydroxyl groups of tetrol **3a** extend in opposite directions, which may be expected to assemble with hydrogen bond acceptors into highly ordered molecular scaffolds. Some nitrogen acceptors were then added into an ethanol solution of **3a**, yielding crystalline adducts after a few days.[10a] In the molecular structure of the 1:1 adduct of 4,4′-bipyridyl and (±)-**3a**, **3a** exists in a dimeric form through two O−H···O hydrogen bonds, and such

(21) (a) Frisch, M. J.; et al. *Gaussian 98*, Revision A.11; Gaussian, Inc.: Pittsburgh, PA, 2001. (b) Wadt, W. R.; Hay, P. J. *J. Chem. Phys.* **1985**, *82*, 284−298. (c) Becke, A. D. *Phys. Rev.* **1988**, *A38*, 3098−3100. (d) Becke, A. D. *J. Chem. Phys.* **1993**, *98*, 1372−1377, 5648−5652. (e) Lee, C.; Yang, W.; Parr, R. G. *Phys. Rev.***1988**, *B37*, 785−789. (d) See the Supporting Information.

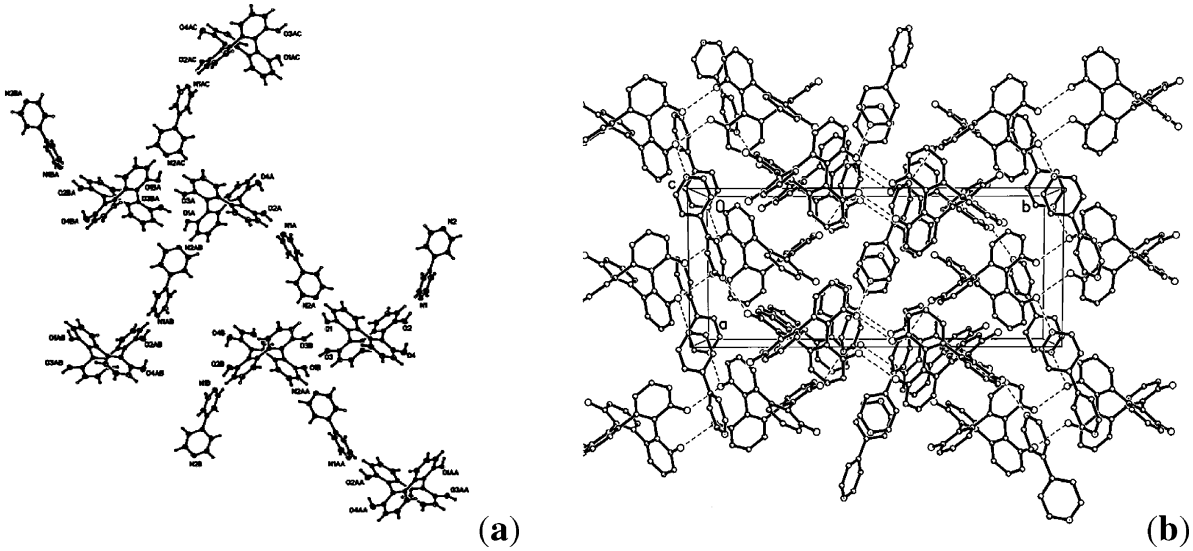

Figure 6. (a) A perspective view of the molecular aggregate of the 1:1 adduct of 4,4′-bipyridyl and (±)-**3a**. (b) A perspective view of crystal packing (viewed down the *c* axis).

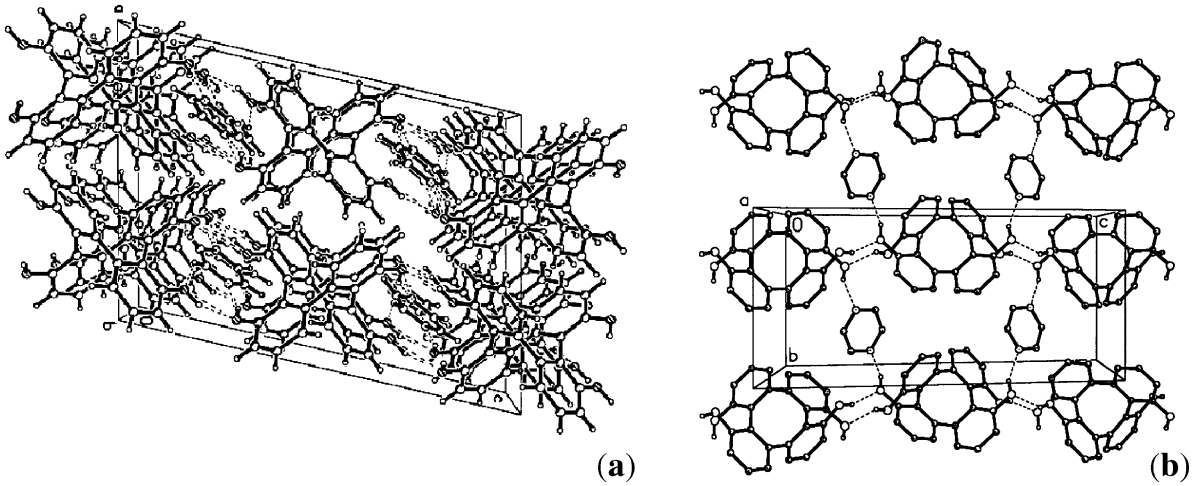

Figure 7. 1:1 adduct of pyrazine and (±)-**3a**. (a) A perspective view of crystal packing (viewed down the *c* axis). (b) Hydrogen-bonded layer in the crystal structure of (±)-**3a**·$C_4H_4N_2$. The tetrol molecules are linked by pairs of O−H···O hydrogen bonds into a chain running parallel to the *c* axis, and such chains are cross-bridged by O−H···N hydrogen bonds (pyrazine molecules as acceptors) to form a corrugated layer. For clarity all hydrogen atoms have been omitted except those of the hydroxyl groups.

Scheme 7

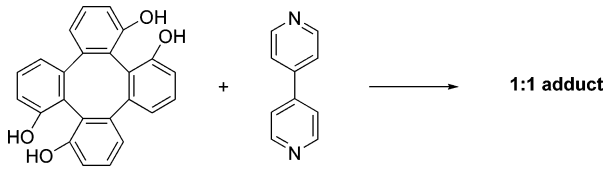

dimers are linked by 4,4′-bipyridyl through O−H···N hydrogen bonds, as shown in Scheme 7 and Figure 6. The same adduct was also obtained from THF and MeOH−toluene.

From Figure 6, it can be concluded that (1) the two tetrol molecules of one dimer are enantiomers and (2) these dimers are not hydrogen bond saturated. They are separate from each other and do not hydrogen bond to those close to them. If each dimer links with two neighboring ones, chains will be composed. So two questions arise: (1) Is the molecule of dipyridyl too long to link the dimers, which makes the dimers (close in space) far from hydrogen bonding? Are shorter molecules (such as pyrazine) suitable to act as linker? (2) What will happen if optically pure **3a** is used? Are there any dimers formed from the same enantiomeric tetrol and linked into double helical chains?

The answer to the first question is yes. A 1:1 adduct was obtained from the mixture of pyrazine and (±)-**3a** in ethanol solution, whose structure was determined by NMR and X-ray studies. Dimers composed by two heterochiral molecules form hydrogen bonds with each other, which result in parallel chains, while pyrazine acts as a linker between adjacent dimers (Scheme 8 and Figure 7).

Notably, the hydroxyl groups hydrogen bonding with nitrogens of pyrazine are on the C-1 and C-8 positions, being different from those on the C-1 and C-9 positions with 4,4′-bipyridyl.

In the 1:1 adduct of 5,5′-dipyrimidine and (±)-**3a**, only two nitrogens of the four of 5,5′-dipyrimidine formed hydrogen bonds with the hydroxyl groups of **3a**. The hydroxyl groups hydrogen bonding with nitrogens of 5,5′-dipyrimidine are on the C-1 and C-8 positions. Self-assembly of homochiral tetrol

Scheme 8

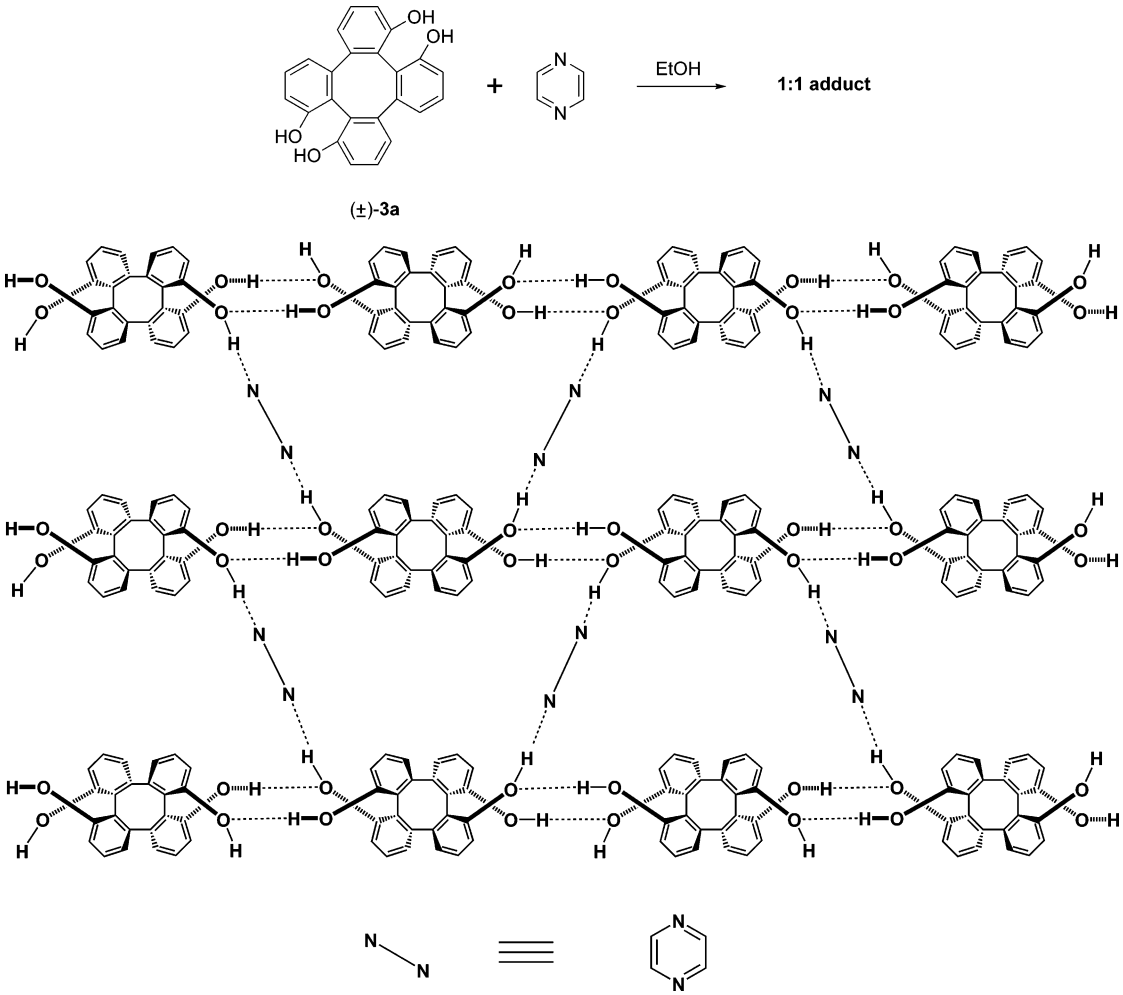

Scheme 9

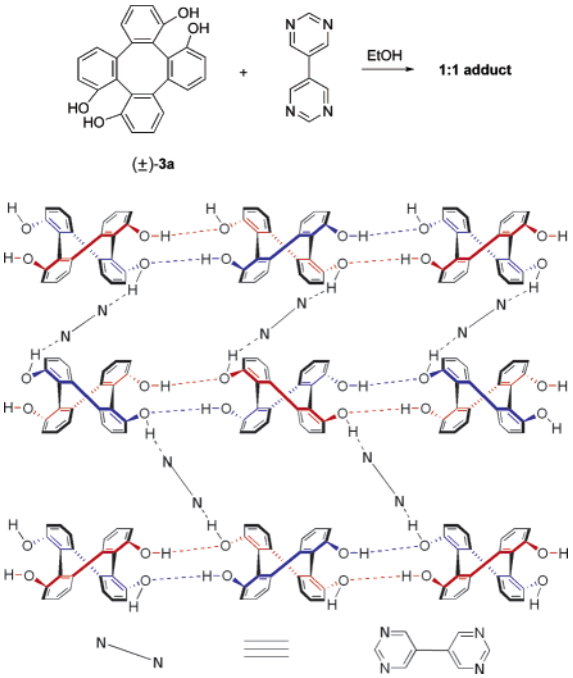

molecules gives parallel chains, while 5,5′-dipyrimidine molecules array as linear linkers between these parallel chains, as depicted in Scheme 9.

The homochiral tetrol molecules are linked by pairs of O−H···O hydrogen bonds into a chiral double helical chain running parallel to the *a* axis, and adjacent chains of opposite chirality are cross-bridged by O−H···N hydrogen bonds to form a corrugated layer, as shown in Figure 8.

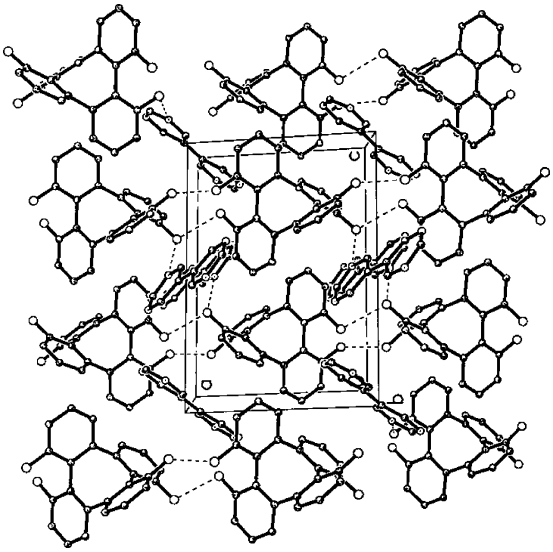

Figure 8. A perspective view of crystal packing of the 1:1 adduct of 5,5′-dipyrimidine and (±)-**3a** (viewed down the *b* axis).

Scheme 10

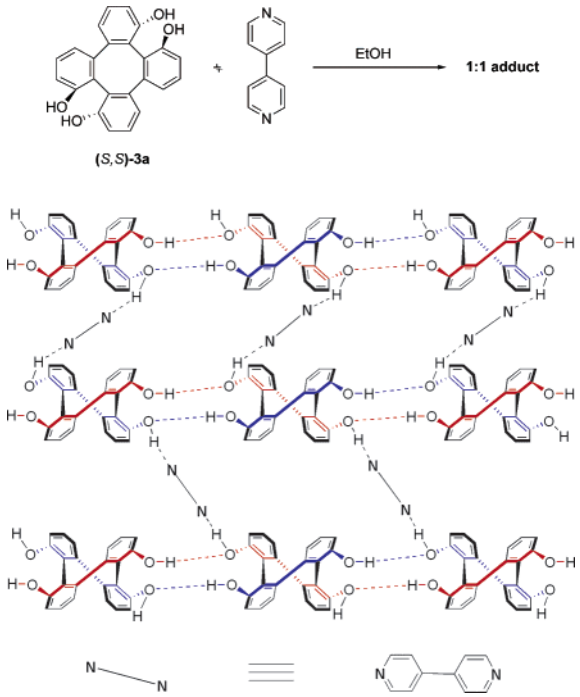

Scheme 11

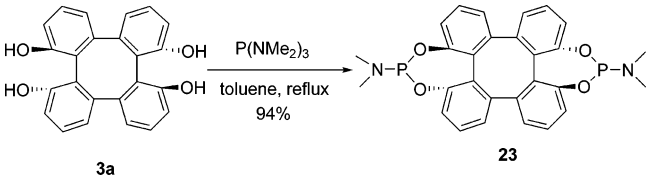

The answer to the second question is also yes. In the 1:1 adduct of (*S*,*S*)-**3a** with 4,4′-dipyridyl, the latter serves as a linker between parallel chiral double helical chains formed by self-assembly of (*S*,*S*)-**3a**, as shown in Scheme 10 and Figure 9. The same result from (*R*,*R*)-**3a** and 4,4′-dipyridyl also confirmed such an arrangement.

From Figure 9b, it can be seen that the tetrol molecules are linked by pairs of O−H···O hydrogen bonds into a chiral double helical chain running parallel to the [101] axis, and such chains are cross-bridged by O−H···N hydrogen bonds (4,4′-dipyridyl molecules as acceptors) to form a corrugated layer (see Figure 9a).

The shorter acceptor, pyrazine, reacted with (*S*,*S*)-**3a** or (*R*,*R*)-**3a**, resulting in 1:1 adducts. Unfortunately, no crystals were obtained from the mixture of pyrazine and optically pure **3a** under the same conditions. Self-assembly of 5,5′-dipyrimidine and optically pure **3a** is under way.

Asymmetric Hydrogenation of Olefins. Early examples concerning asymmetric transition-metal-catalyzed hydrogenation reactions of prochiral olefins were reported independently by Horner[22a] and Knowles[22b] in 1968. The ligands used are chiral monophosphanes, but low ee values were obtained. A larger number of bidentate ligands with excellent selectivities, such as CAMP[23] and BINAP,[24] were subsequently designed and tested. Recently monodentate phosphite and phosphoramidites were reported by Pringle[25] and Feringa[26] which showed high enantioselectivities in the rhodium-catalyzed hydrogenation of acetamidocinnamate. Encouraged by these results, a novel linear ligand (**23**) based on **3a** was designed, and was easily prepared in one step from **3a** and hexamethylphosphorus triamide as shown in Scheme 11. The NMR and mass spectroscopies of **23** as well as its element analysis are in full accord with the assigned structure. There is only one signal at δ 145.7 ppm for aminophosphite in its ^{31}P NMR spectrum. The molecular ion peak of compound **23** in its EI mass spectrum was observed at *m*/*z* 514.

The asymmetric hydrogenation of olefin substrate **24** was readily catalyzed by $Rh(COD)_2BF_4$ utilizing (*S*,*S*)-**23** as a ligand (Scheme 12). The hydrogenation reaction of phenyl 2-acetamidocinnamate (**24a**) was performed in CH_2Cl_2 at 15 °C under a H_2 pressure of 20 atm in the presence of 1 mol % Rh catalyst formed in situ from [$Rh(COD)_2BF_4$] and (*S*,*S*)-**23**, resulting in (*R*)-**25** in 95.6% ee. Toluene was found to be not a good solvent for this reaction (Scheme 12, entries 1 and 2), maybe due to the poor solubility of the catalytic species in toluene. A higher pressure of H_2 (30 atm) gave a slightly lower ee value (Scheme 12, entries 1 and 3). A lower pressure of H_2 (10 atm) also resulted in a slightly lower ee value (Scheme 12, entries 5 and 6). Low temperature (0 °C) decreased the conversion to 10%, and only 5% ee was realized (Scheme 12, entry 4). A slightly higher enantioselectivity was obtained when the hydrogenation reaction was carried out at 25 °C (Scheme 12, entry 5).

The asymmetric hydrogenation of various acetamidocinnamate derivatives (**24b**−**e**) was investigated in CH_2Cl_2 at 25 °C under a pressure of 20 atm (Scheme 12, entries 7−10). Higher enantioselectivities were achieved when more sterically hindered or electron-deficient substrates were employed. For all methyl esters, the conversions are quantitative and the enantioselectivities (94.9−99.0% ee) are comparable to those achieved with other monodentate phosphorus ligands and bidentate phosphorus ligands (e.g., CAMP, 90%,[23] BINAP, 67−100%,[24] MonoPHOS, 93.2−99.8%,[26] and SIPHOS, 95.6−99.3%[27]). It is expected that oligomeric or polymeric complexes may form when **23** is allowed to react with 1 equiv of [$Rh(COD)_2BF_4$], although the possibility of forming a square complex cannot be ruled out.[8] We were unable to dissolve the solids that formed in these reactions. This result might be indicative of formation of oligomeric or polymeric mixtures.[28]

Conclusion

In conclusion, we have synthesized chiral 1,8,9,16-tetrahydroxytetraphenylene (**3a**) and 1,8,9,16-tetrakis(diphenylphosphino)tetraphenylene (**3b**). These chiral building blocks were employed to construct two chiral rodlike triblock platinum complexes, (*R*,*R*,*R*,*R*)-**17** and (*S*,*S*,*S*,*S*)-**20**, and one chiral rodlike pentablock complex, (*R*,*R*,*R*,*R*,*R*,*R*,*R*,*R*)-**22**.

(22) (a) Horner, L.; Siegel, H.; Buthe, H. *Angew. Chem.* **1968**, *80*, 1034−1035. (b) Knowles, W. S.; Sabacky, M. J. *Chem. Commun.* **1968**, 1445−1446.
(23) (a) Vineyard, B. D.; Knowles, W. S.; Sabadky, M. J.; Bachman, G. L.; Weinkauff, D. *J. Am. Chem. Soc.* **1977**, *99*, 5946−5952. (b) Knowles, W. S.; Sabacky, M. J.; Vineyard, B. D.; Weinkauff, D. J. *J. Am. Chem. Soc.* **1975**, *97*, 2567−2568.
(24) Miyashita, A.; Yasuda, A.; Takaya, H.; Toriumi, K.; Ito, T.; Souchi, T.; Noyori, R. *J. Am. Chem. Soc.* **1980**, *102*, 7932−7934.
(25) Claver, C.; Fernandez, E.; Gillon, A.; Heslop, K.; Hyett, D. J.; Martorell, A.; Orpen, A. G.; Pringle, P. G. *Chem. Commun.* **2000**, 961−962.
(26) van Berg, M.; Minnaard, A. J.; Schudde, E. P.; van Esch, J.; Vries, A. H. M.; Vries, J. G.; Feringa, B. L. *J. Am. Chem. Soc.* **2000**, *122*, 11539−11540.
(27) Fu, Y.; Xie, J.-H.; Hu, A.-G.; Zhou, H.; Wang, L.-X.; Zhou, Q.-L. *Chem. Commun.* **2002**, 480−481.
(28) Wang, X.; Ding, K. *J. Am. Chem. Soc.* **2004**, *126*, 10524−10525.

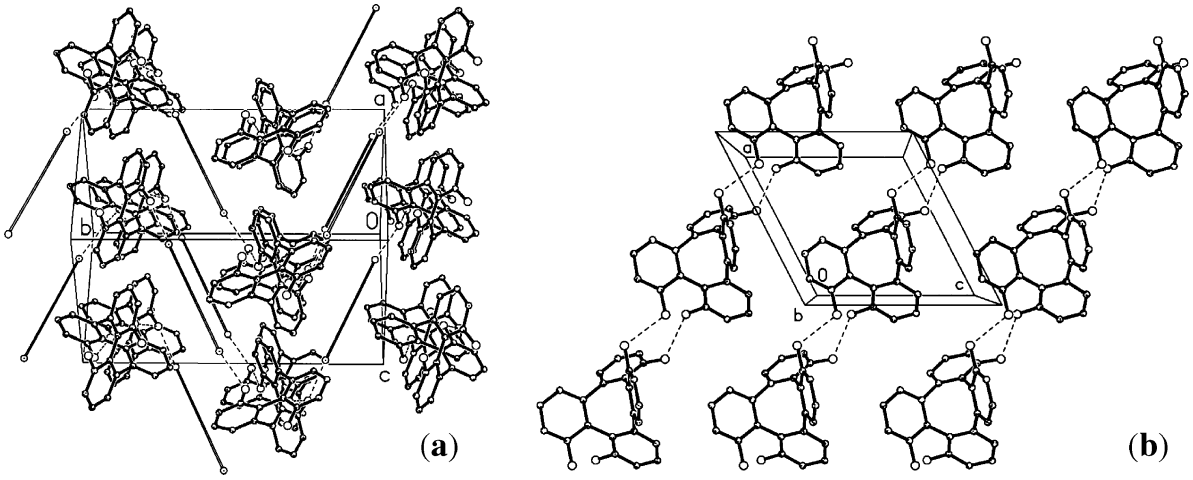

Figure 9. (a) A perspective view of crystal packing of the 1:1 adduct of 4,4′-dipyridyl and (*S*,*S*)-**3a** (viewed down the *b* axis). For simplicity the 4,4′-dipyridyl molecule is represented by a rigid rod. (b) Hydrogen-bonded layer in the crystal structure of (*S*,*S*)-**3a**·$C_{10}H_8N_2$. For clarity all hydrogen atoms have been omitted.

Scheme 12

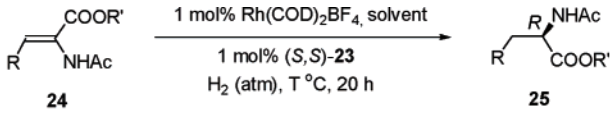

24 **25**

Entry	substrate	R	R′	Solvent	T (°C)	H_2 (atm)	Conv. (%)	Ee (%)
1	**24a**	C_6H_5	Me	CH_2Cl_2	15	20	100	95.6 (*R*)
2	**24a**	C_6H_5	Me	toluene	15	26	66	7 (*R*)
3	**24a**	C_6H_5	Me	CH_2Cl_2	15	30	100	95.0 (*R*)
4	**24a**	C_6H_5	Me	CH_2Cl_2	0	20	10	5 (*R*)
5	**24a**	C_6H_5	Me	CH_2Cl_2	25	20	100	96.9 (*R*)
6	**24a**	C_6H_5	Me	CH_2Cl_2	25	10	100	95.2 (*R*)
7	**24b**	H	Me	CH_2Cl_2	25	10	100	94.9 (*R*)
8	**24c**	Me	Me	CH_2Cl_2	25	20	100	95.7 (*R*)
9	**24d**	4-ClC_6H_4	Me	CH_2Cl_2	25	20	100	98.8 (*R*)
10	**24e**	4-$NO_2C_6H_4$	Me	CH_2Cl_2	25	20	100	99.0 (*R*)

There are no intermolecular hydrogen bonds involving the hydroxyl groups of **3a**, except that they form hydrogen bonds with the solvent molecules. Highly ordered structures were obtained when linear acceptors formed hydrogen bonds with **3a**. In the 1:1 adduct of 4,4′-bipyridyl and (±)-**3a**, tetrol **3a** existing in a dimeric form is linked by 4,4′-bipyridyl through hydrogen bonds. Pyrazine serves as a short linker between achiral parallel chains each formed by (±)-**3a**, while self-assembly of homochiral tetrol molecules into alternate parallel chains occurs in the adduct of 5,5′-dipyrimidine with (±)-**3a**. Self-assembly of (*S*,*S*)-**3a** or (*R*,*R*)-**3a** with 4,4′-dipyridyl yielded a packing of chiral double helical chains formed by chiral tetrol molecules.

An effective linear chiral ligand, (*S*,*S*)-**23**, has been developed for the catalytic hydrogenation of acetamidocinnamate derivatives. This is the first example of a chiral tetraphenylene derivative being used as an effective catalytic hydrogenation ligand. The high enantioselectivity (up to 99% ee) and stability may indicate the potential of tetraphenylene derivatives in asymmetric catalysis.

Acknowledgment. This work was supported by grants from the Research Grants Council of the Hong Kong Special Administrative Region, China (Project CUHK 4264/00P), and the Croucher Foundation (Hong Kong). H.-Y.P. acknowledges with thanks the Croucher Foundation (Hong Kong) for a Shanghai Studentship. The Science and Technology Commission of the Shanghai Municipality also partially supported this program. We thank Professor Li-Xin Dai and Xue-Long Hou for helpful discussions and Dr. Xi-Cheng Dong for molecular models.

Supporting Information Available: Experimental details, computation results, X-ray crystallographic data of **3a**, **10**, **13**, **15**, and adducts of **3a** with acceptors, CD spectrum of (*S*,*S*)-**3a** and (*R*,*R*)-**3a**, and complete ref 21a. This material is available free of charge via the Internet at http://pubs.acs.org.

JA051013L